Journal of Power Sources 196 (2011) 4200–4208

Contents lists available at ScienceDirect

Journal of Power Sources

journal homepage: www.elsevier.com/locate/jpowsour

Catalyst layers for proton exchange membrane fuel cells prepared by electrospray deposition on Nafion membrane

A.M. Chaparro[a,*], P. Ferreira-Aparicio[a], M.A. Folgado[a], A.J. Martín[a], L. Daza[a,b]

[a] *CIEMAT, Avda. Complutense 22, 28040 Madrid, Spain*
[b] *Instituto de Catálisis y Petroleoquímica (CSIC), C/Marie Curie 2, Campus Cantoblanco, 28049 Madrid, Spain*

ARTICLE INFO

Article history:
Received 28 July 2010
Received in revised form
20 September 2010
Accepted 29 September 2010
Available online 7 October 2010

Keywords:
PEMFC
Electrospray
Catalyst layer
Cathode
Nafion
Pt/C

ABSTRACT

The electrospray deposition method has been used for preparation of catalyst layers for proton exchange membrane fuel cells (PEMFC) on Nafion membrane. Deposition of Pt/C + ionomer suspensions on Nafion 212 gives rise to layers with a globular morphology, in contrast with the dendritic growth observed for the same layers when deposited on the gas diffusion layer, GDL (microporous carbon black layer on carbon cloth) or on metallic Al foils. Such a change is discussed in the light of the influence of the Nafion substrate on the electrospray deposition process. Nafion, which is a proton conductor and electronic insulator, gives rise to the discharge of particles through proton release and transport towards the counter electrode, compared with the direct electron transfer that takes place when depositing on an electronic conductor. There is also a change in the electric field distribution in the needle to counter-electrode gap due to the presence of Nafion, which may alter conditions for the electrospray effect. If discharging of particles is slow enough, for instances with a low membrane protonic conductivity, the Nafion substrate may be charged positively yielding a change in the electric field profile and, with it, in the properties of the film. Single cell characterization is carried out with Nafion 212 membranes catalyzed by electrospray on the cathode side. It is shown that the internal resistance of the cell decreases with on-membrane deposited cathodic catalyst layers, with respect to the same layers deposited on GDL, giving rise to a considerable improvement in cell performance. The lower internal resistance is due to higher proton conductivity at the catalyst layer-membrane interface resulting from on-membrane deposition. On the other hand, electroactive area and catalyst utilization appear little modified by on-membrane deposition, compared with on-GDL deposition.

1. Introduction

Electrospray ionization occurs when a liquid or suspension is ejected under the influence of a strong electric field [1–3]. The electrospray effect may be applied to preparation of the catalyst layers for proton exchange membrane fuel cells (PEMFC), through the ejection of suspensions containing the catalyst (platinum nanoparticles supported on carbon black, Pt/C) and the ionomer (Nafion) on a substrate. Deposition occurs by this way under special conditions, mostly involving electrostatic interactions among catalyst particles, ionomeric phase and the substrate. As a result, the electrosprayed films show particular properties, like a dendritic (ramified) morphology, high mesoporosity and stronger catalyst–ionomer interaction [4–6]. Single cell performance is improved with electrodes prepared by electrospray, showing a decrease in the internal resistance and higher catalyst utilization when compared with electrodes prepared by other methods, like the airbrushing, or commercial electrodes [6].

For preparation of PEMFC electrodes, the electrospray deposition of the catalyst layer is normally carried out on the gas diffusion layer (GDL), consisting of a microporous carbon black layer on top of a carbon cloth. This appears to be, in principle, the most appropriate procedure because the GDL is easy to handle, robust, and may be submitted to thermal treatments above 100 °C that may be necessary to optimise properties of the deposited catalyst layers. In addition, the GDL is a good electronic conductor so the charged catalyst particles arriving to the substrate may discharge by direct electron transfer, which is a necessary step in electrospray deposition. The process requires passing of a dc current, with ionic conduction in the tip to substrate gap (i.e. liquid meniscus and aerosol phase), and electronic conduction in the rest of the circuit (Fig. 1). It is obvious to infer many similarities between the electrospray deposition and a typical electrochemical deposition process [1,7]: in both cases, a current is generated by electrochemical reactions at an anode and a cathode, which is proportional to the growth of the film. Particular characteristics of the electrospray deposition of catalyst layers will be further commented in the discussion.

---

* Corresponding author at: CIEMAT, Fuel Cells Group, Avda. Complutense 22, 28040 Madrid, Spain. Tel.: +34 913460897; fax: +34 913466604.
E-mail address: antonio.mchaparro@ciemat.es (A.M. Chaparro).

0378-7753/$ – see front matter © 2010 Elsevier B.V. All rights reserved.
doi:10.1016/j.jpowsour.2010.09.096

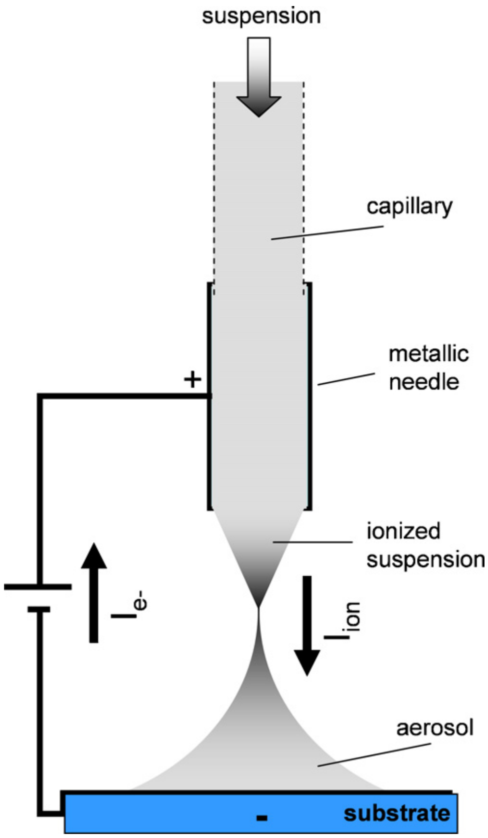

Fig. 1. Scheme of the electrospray deposition process. Parts are drawn at different scales for better detail.

The electrospray deposition on-membrane, instead of on-GDL, is another possibility of interest for the preparation of PEMFC electrodes. It is well known that on-membrane deposition of the catalyst layer usually improves the performance of PEMFC electrodes due to better contact between the catalyst layer and the membrane [8–10]. On the other hand, the membrane (Nafion) as substrate sets some practical difficulties for catalyst layer deposition, requiring very careful handling to avoid deformation and pinholes, film adherence may be difficult to attain on its surface, and, in addition, it is not appropriate for post-deposition thermal treatments. For these reasons, procedures for preparation of catalyst layer on-membrane may require a transfer step between a different deposition substrate and the membrane ('decal' method). The electrospray deposition may be an alternative method of interest for the direct deposition of the catalyst layers on-membrane. Mostly, the electrosprayed particles and the ionomer arrive free of solvent to the substrate, and deposit under electrostatic interaction displaying an appropriate porosity network. In this work, the electrospray deposition of Pt/C + ionomer catalyst layers on Nafion membrane is explored. The viability of the procedure is demonstrated. Further, the influence of the Nafion membrane on the electrospray process is discussed. The resulting catalyst films are characterized by SEM microscopy and evaluated in single PEMFC, and compared with the properties of 'on-GDL' deposited catalyst layers.

2. Experimental

Suspensions of Pt/C + ionomer (Nafion) have been prepared from commercial platinum on carbon catalyst (Pt/C, E-TEK, 20 wt% platinum), Nafion solution (Aldrich, 5%), and isopropanol (Panreac) as solvent. The amount of Pt in the electrodes was 0.21 mg cm^{-2}, and Nafion was added in 15 wt% proportion of catalyst layer, which is the optimal amount determined in previous works [5]. Suspensions are submitted to ultrasonic stirring for two hours before the deposition for homogenization and disruption of larger agglomerates. The setup for electrospray deposition has been described in previous works [6]. Briefly, a high dc voltage (4–9 kV) is applied between the ejector needle and the substrate. The Pt/C + Nafion suspension flows through a silica capillary, 150 μm internal diameter, at a rate of 20 μl min^{-1}, under a small nitrogen overpressure (0.1–0.2 bar). The deposition substrate, either the GDL (ELAT E-TEK, LT1200W, PEMEAS) or the Nafion membrane (NR-212, 50.8 μm thickness, 0.92 meq g^{-1} acid capacity), is placed on a metalized *x*–*y* stage, which is at the same time the counter electrode. A platinum foil electrode is placed underneath, between the substrate and the counter electrode, to improve the conductivity. During deposition, the temperature of the suspension is maintained at 22 °C, and that of the counter electrode at 50 °C. The measured electrospray current was typically 1–10 nA (Picoammeter, Keithley), and the area of electrospray deposited catalyst layers was 4 cm × 4 cm. SEM images of Pt/C + ionomer films deposited on different substrates (Nafion 212, GDL, and Al foil) were taken with Hitachi 2500, using Au contact evaporated on the sample.

The performance of catalyzed membranes (only on the cathode side) and catalyzed GDL (cathodic) was compared in single PEMFC. With this aim, the single cells were mounted using commercial anode electrode (ELAT E-TEK LT120EWALTSI, 0.25 mgPt cm^{-2}, with Pt/C catalyst 30 wt% on Vulcan XC72R); gas distribution was carried out through graphite plates with two channels, serpentine, flow field; the current collectors were gold plated copper plates, and the stainless steel end plates had heating resistors to maintain cell temperature. Silicone gaskets were placed between the different layers. After cell mounting, standard leakage and crossover tests were carried out on the single cells. Testing was carried out using home made stations, with mass flow controllers for oxygen and hydrogen inlet, heated pipes, backpressure control, and humidifiers. Current drawn from the cell is controlled with an electronic load (HP 6060B). A software in Labview allows for voltage and high frequency resistance (1 kHz, Agilent 4338B) to be continuously monitored.

Single cell operation was carried out following a standard protocol. Cell is started up by increasing the current demand in 100 mA steps, up to 1 A, and then temperature of the cell and humidifiers are conditioned at 80 °C. Once constant voltage and high frequency internal resistance are attained, usually after 12–24 h steady-state operation, polarization curves are measured under normalized conditions: H_2/O_2 flow, 1.5/3.0 ($\lambda_{H_2}/\lambda_{O_2}$) constant stoichiometry, 1 atm gauge pressure, 100% humidification, and 80 °C cell temperature. For the acquisition of the polarization curves, the current demand is fixed at different values, from high to low values in 1 A steps, together with the corresponding H_2 and O_2 flows; at each current demand, the voltage and the internal resistance are measured after constant, steady, values are attained, usually after 5–10 min of fixing the current demand. The electroactive area of the cathodic catalyst layers was measured from the desorption charge of the underpotentially adsorbed hydrogen, under H_2/N_2 flow (30/30 ml min^{-1}) in anode/cathode, at 30 °C. Measurements were carried out at different sweep rates, and the maximum desorption charge was taken as the closest value to the real electroactive area [11]. For area calculation, the conversion factor 210 μC cm^{-2} was applied.

3. Results

3.1. Morphology of the films

A photograph of a typical Pt/C + Nafion film deposited by electrospray on Nafion 212 membrane is shown in Fig. 2. The films

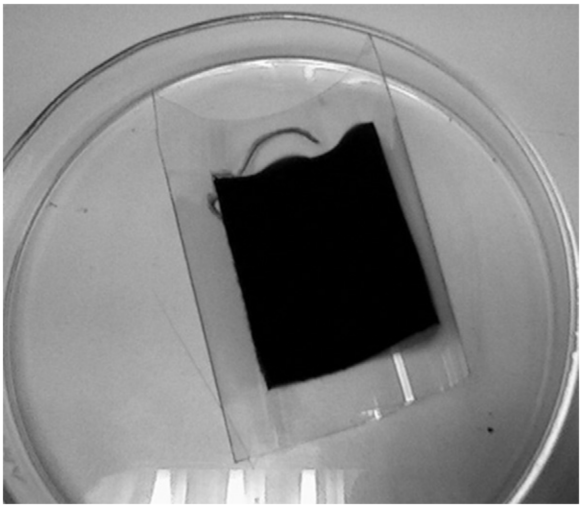

Fig. 2. Photograph of a Nafion membrane covered with a Pt/C + Nafion catalyst layer by electrospray deposition.

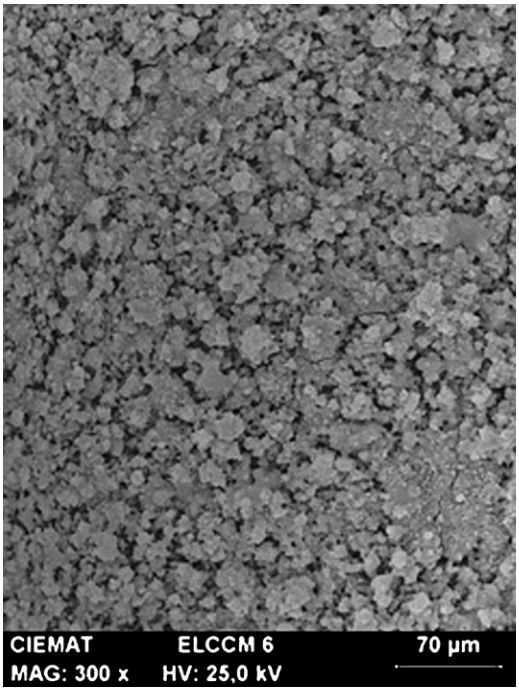

Fig. 3. SEM image of a Pt/C + Nafion catalyst layer deposited on Nafion membrane.

show rather good adherence, enough to maintain integrity during manipulations following deposition and mounting the single cell. The microscopic morphology of the films was analysed with SEM (Figs. 3–5). Fig. 3 shows SEM image at low magnification (300×) of a Pt/C + Nafion film. The films present highly porous, free of cracks, morphology at this scale, with a regular formation of aggregates. Such regular disposition of the aggregates is also observed in electrospray deposited layers on GDL substrate (cf. Fig. 2a and b in Ref. [6]). Fig. 4 compares the morphology of the same film at two different levels, one corresponding to layers in contact with the membrane (Fig. 4a and b), and the other is the top surface of the film (Fig. 4c and d). It is observed that layers in contact with the membrane are more irregular, with smaller agglomerates and some dendritic growth, whereas morphology of the surface of the film is softened and the size of agglomerates increases, showing now globular growth type.

Fig. 5 compares the surface morphology of Pt/C + Nafion films deposited on different substrates: Nafion membrane (Fig. 5a and b), commercial GDL (Fig. 5c and d), and aluminium foil (Fig. 5e and f). The film deposited on the membrane shows the globular morphology and spherical agglomerates commented above in Fig. 4c and d (top surface morphology). Deposition on GDL and Al foil substrates gives rise, on the other hand, to a different morphology, with higher ramification of aggregates (Fig. 5c–f).

3.2. Single cell testing

Polarization curves corresponding to two single cells with electrospray deposited cathode catalyst layers, on-membrane and on-GDL, are compared in Fig. 6a. A significant improvement in the response is found for on-membrane deposited film, mostly at current demands above 0.5 A cm^{-2}. The same figure shows the high frequency (1 kHz) resistance of the cells, which shows values around 75 mΩ cm^2 for the cell with the on-membrane cathodic layer, whereas with on-GDL deposited layer the resistance is practically doubled.

Polarization curves have been analysed by fitting to the equation:

$$V = E^0 - b \cdot \log\left(\frac{i}{i_0}\right) - i \cdot R_i \qquad (1)$$

where V (V) is cell voltage, E^0 (V) is the thermodynamic potential at p = 2 atm and 353 K (1.19 V), i (A cm^{-2}) the current density, i_0 (A cm^{-2}) the exchange current density, and R_i the dc internal resistance. Table 1 shows the parameter values resulting from the analysis. It is obtained that the parameters characteristic of the catalytic activity (i_0 and b) are very similar for both on-membrane and on-GDL deposition. However, the calculated internal resistance is about 30% lower for on-membrane deposited catalyst layer. The difference in the internal resistances, which are dc resistances, is similar to those experimentally measured at 1 kHz (Table 1), indicating that fast conducting mechanisms have improved when depositing on membrane. These mechanisms must correspond to proton conduction at the cathode–membrane interface, provided other fast contributions should not be altered by changing the deposition substrate, like conduction in the membrane (protonic) and the cathode (protonic and electronic) [12]. Power density curves (Fig. 6b) show about 25% improvement at the maximum value for the cell mounted with the on-membrane deposited cathodic layer, as a consequence of the lower internal resistance.

The active area of the electrodes was measured by the hydrogen desorption charge method. Fig. 7 shows the dependence of the hydrogen desorption charge with voltage sweep rate. The area is calculated from the maximum value of the desorption charge, which is less affected by interfering processes during the voltammetry, mainly carbon substrate reactivity and the adsorption of carbon species [11]. It is obtained very similar electroactive area

Table 1
Parameters corresponding to best fit of polarization curves in Fig. 6 to Eq. (1). Also indicated the specific area, roughness factor, and high frequency resistance measured at 1 kHz.

Substrate	Specific area (m^2 g$_{Pt}$$^{-1}$)	Roughness factor	$i_0 \times 10^7$ (A cm^{-2})	b (mV dec^{-1})	R_i (dc) (mΩ cm^2)	R_i (1 kHz) (mΩ cm^2)
Membrane	46	97	1.3 ± 0.6	62 ± 2	182 ± 3	71
GDL	44	92	1.9 ± 0.9	59 ± 2	263 ± 3	164

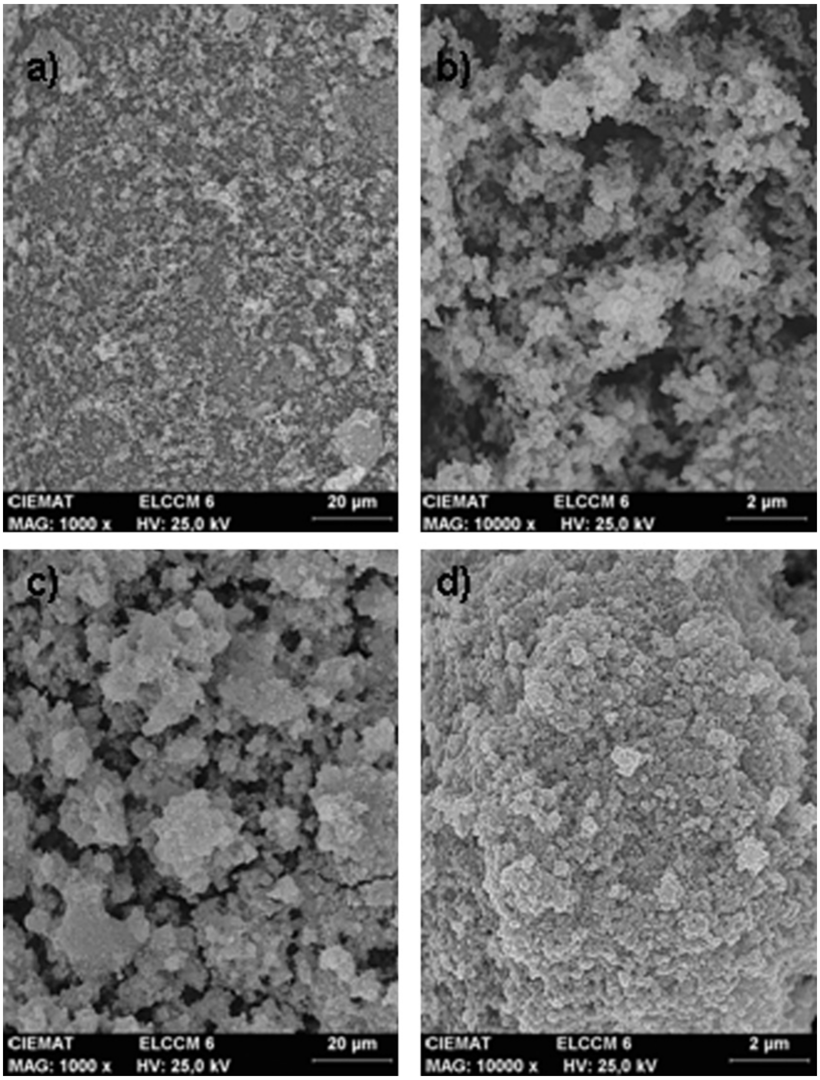

Fig. 4. SEM images of a Pt/C + Nafion film deposited by electrospray on Nafion membrane. (a and b) Images of the layer in contact with the membrane; (c and d) images of the surface layer of the film.

for both catalyst layers, deposited on membrane and on GDL. The specific area is 45 m^2 g_{Pt} which is typically higher than values measured with electrodes prepared by other methods (airbrushing) and commercial electrodes, normally in the range of 20–30 m^2 g_{Pt} according to our area measuring procedure.

4. Discussion

It is shown that the electrospray deposition ‘on-membrane’ gives rise to catalyst films with rather good adherence. The catalyst layers on-membrane have a globular surface morphology, compared with more dendritic growth of the same layers deposited on the GDL or Al foil substrates. It is also observed for films deposited on membrane a change in the morphology from the layers deposited directly on the membrane to those on the surface of the film. It is of interest first to discuss morphology changes of catalyst layers in view of the differences that the Nafion substrate introduces in the electrospray process.

4.1. Analysis of the electrospray deposition on membrane

The electrospray deposition has close similarities with a deposition process in a conventional two-electrode electrochemical cell. During deposition, electrochemical reactions take place both at the ejector needle and at the substrate, and an ionic conducting path is established between the ejector and the substrate that includes a liquid phase part, inside the meniscus, and a gas phase part in the aerosol. As a consequence, a dc current flows proportional to the deposition rate (Fig. 1). In the electrospray deposition, the electrochemical equivalent, i.e. mass deposited per mol of charge, is not a precise concept because the mass and charge of depositing units (particles) depend on different parameters, like surface chemistry and composition of particles, solvent composition, and the ionization parameters (dc voltage, flow rate, ejector geometry, among others). It has been observed that the charge to mass ratio for electrospray deposition of a liquid is inversely proportional to the size of generated droplets [13]. For deposition of Pt/C catalyst an average of 2 elementary charges per single particle is estimated when deposition occurs under 1 nA current and a suspension flow rate is 20 $\mu l\ min^{-1}$, and considering that Nafion chains remain uncharged. It means that multiply charged particles is a probable situation during electrospray deposition of catalyst layers, which favours particles deagglomeration and the interaction with the ionomer [6].

During electrospray under positive ionization mode, oxidative reactions take place at the ejector that yield positive ions

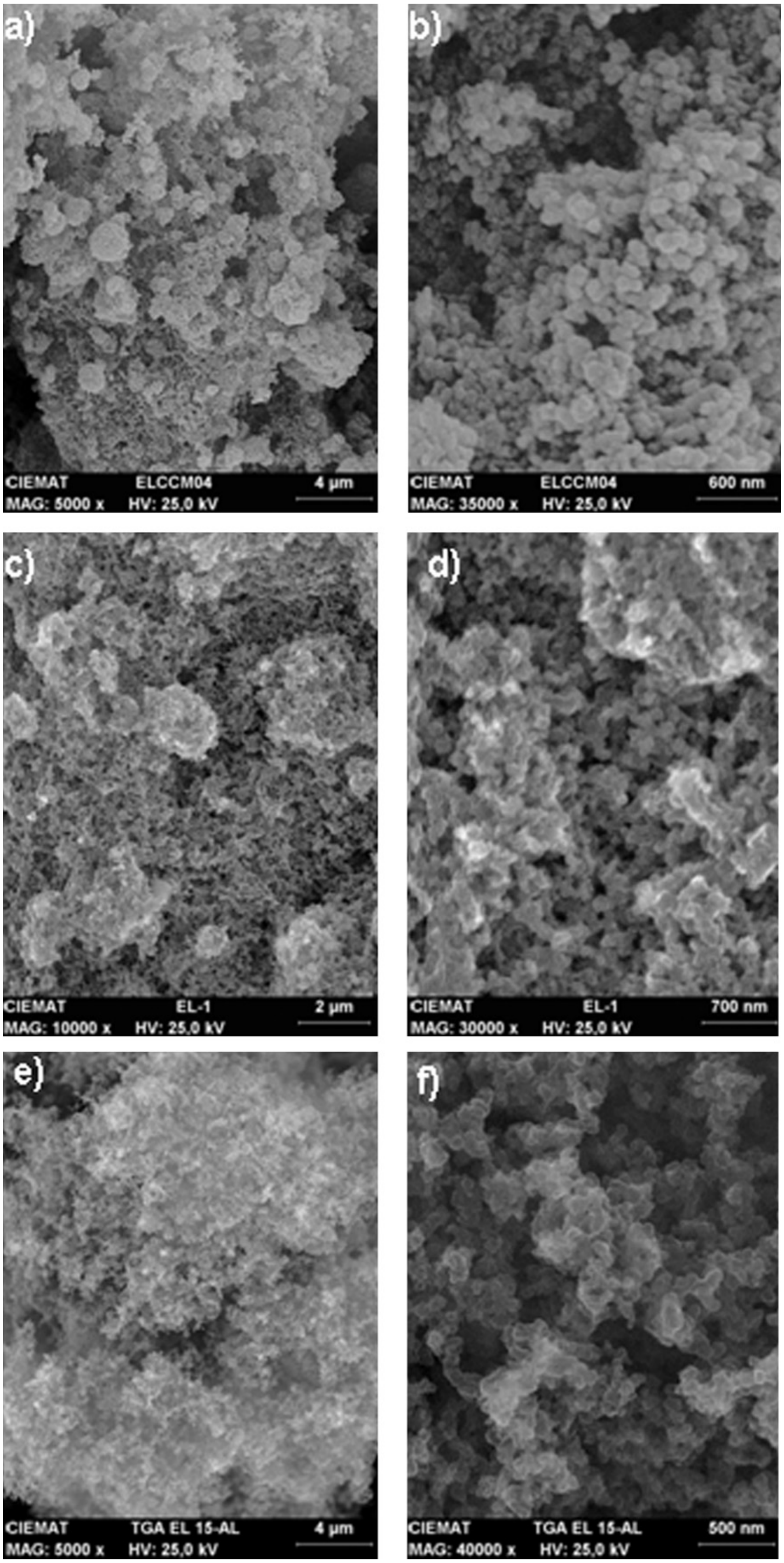

Fig. 5. SEM images of Pt/C + Nafion catalyst layers deposited by electrospray on Nafion N212R (a and b), a commercial GDL (c and d), and an aluminium foil (e and f).

by the electrochemical oxidation of components of the catalyst suspension. The reactions are driven by the interfacial potential established between the ejector and the suspension, which depends on variables like ionization potential, current density, concentration of species, ejector material and geometry [7]. The reactions are mostly related with the oxidation of solvent species, ie. isopropanol and water:

$$CH_3CH_2OCH_3 + 5H_2O \rightarrow 18H^+ + 3CO_2 + 18e^- \quad (2)$$

$$H_2O \rightarrow 2H^+ + 0.5O_2 + 2e^- \quad (3)$$

Charging of catalyst particles takes place following reactions (2) and (3), by protons reaction on basic sites of the Pt/C particles surface and Nafion sulphonic groups:

$$[P]\text{–}B: + H^+ \rightarrow [P]\text{–}BH^+ \quad (4)$$

$$[Nf]\text{–}O\text{–}CF_2\text{–}CF_2\text{–}SO_3{}^- + H^+ \rightarrow [Nf]\text{–}O\text{–}CF_2\text{–}CF_2\text{–}SO_3H \quad (5)$$

where [Nf] and [P] represent Nafion moiety and catalyst particles, respectively. [P]–B: represents a generic basic site on the surface of carbon which charges positively under reaction with a proton (reaction (4)). It is to be expected that ionization of particles will be very dependent on the concentration and type of functional groups on carbon. According to a recent study with XPS, O and N heteroatoms are in 1 at.% concentrations on the surface of untreated carbon blacks [14]. The oxygen functionality corresponds to C=O quinone type groups, C–OH phenolic and/or C–O–C ether groups, and C–OOH carboxylic groups and/or water, respectively, whereas nitrogen functionality corresponds to (by order of abundance) pyridinic (N-6) > pyrrolic/pyridone (N-5) > quaternary (N-Q) > pyridine-N-oxide (N-X). The functional groups give a general electronegative character to the surface of carbon blacks, causing proton uptake activity at neutral and acidic pH in the range of 0.2–0.4 mmol g^{-1} [14]. On the other hand, a study with XPS and SIMS [15] shows that also sulphur functional groups (HS^-, SO_x, HSO_x, SCN^-, etc.) appear in 0.4 at.% on the surface of Vulcan XC72. During electrospray, the positive ionization of particles at the ejector needle is caused by the reactions of protons on Lewis basic sites (electron pair donors) associated to most surface nitrogen groups and some of the oxygen and sulphur groups (ethers, ketones, quinone and sulphoxides).

The ionized particles migrate within the suspension towards the surface of the meniscus, which acquires a typical inverted cone shape due to different forces acting, electric, surface tension, gravity and viscosity [16]. At the apex of the cone, the suspension is drawn to a jet of positively charged droplets which breaks up into droplets due to the mutual repulsion of charges overcoming the surface tension (Rayleigh limit) [17]. By this means, the ejection of suspension components (Pt/C particles, Nafion and solvent) gives place to an aerosol mist of charged droplets.

In the aerosol, the second part of the ionic conducting path during electrospray, suspension droplets continue migration towards the substrate, and may be submitted to different processes. Solvent molecules evaporate, leaving free ionized catalyst particles surface and ionomer chains. A specific interaction between sulphonic groups of Nafion and platinum is possible at this stage, as reflected by analysis of thermal decomposition of electrosprayed layers presented in a previous paper [6]. Such Pt–Nafion (sulphonic groups) interaction is relevant to explain the high electroactive area and low ionic resistance of electrospray deposited catalyst layers. On the other hand, there also exists the possibility of disruption of weak interactions in the aerosol phase, mostly non-covalent, due to collisions among particles and ionomer chains. It is known from mass spectrometry analysis that large molecules and polymers may dissociate by breaking of soft covalent bonds (‘collisionally activated dissociation’) [3,18]. In the Pt/C + Nafion mist, collisions may give rise mostly to the complete deagglomeration of catalyst particles

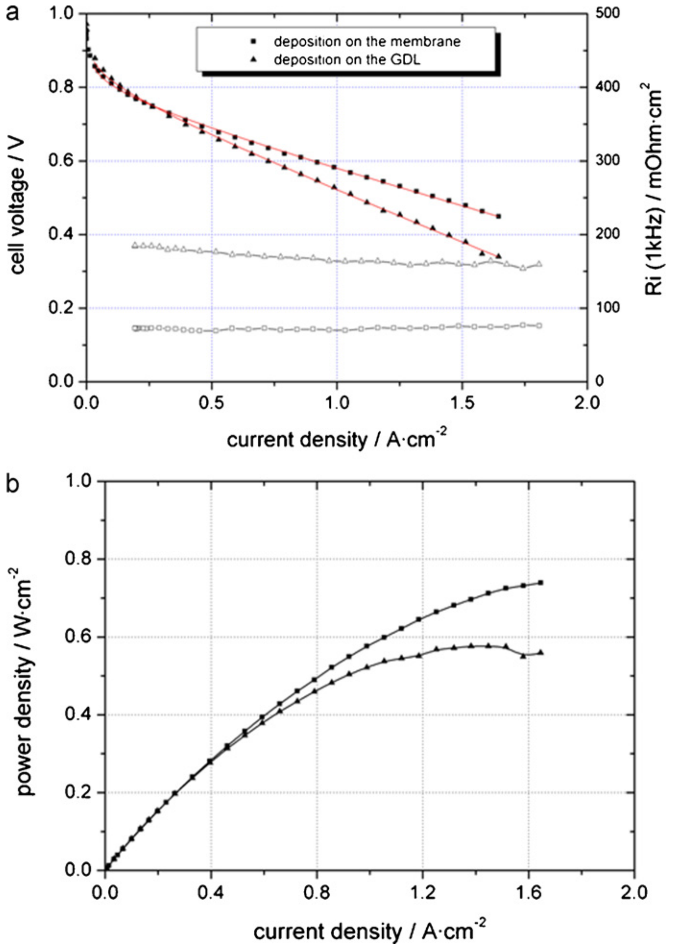

Fig. 6. (a) Polarization curves and high frequency internal resistance, corresponding to two single PEMFC with cathodic catalyst layers deposited by electrospray on membrane and on GDL, respectively. Red lines correspond to theory curves (Eq. (1)). (b) Power density curves. (For interpretation of the references to color in this figure legend, the reader is referred to the web version of the article.)

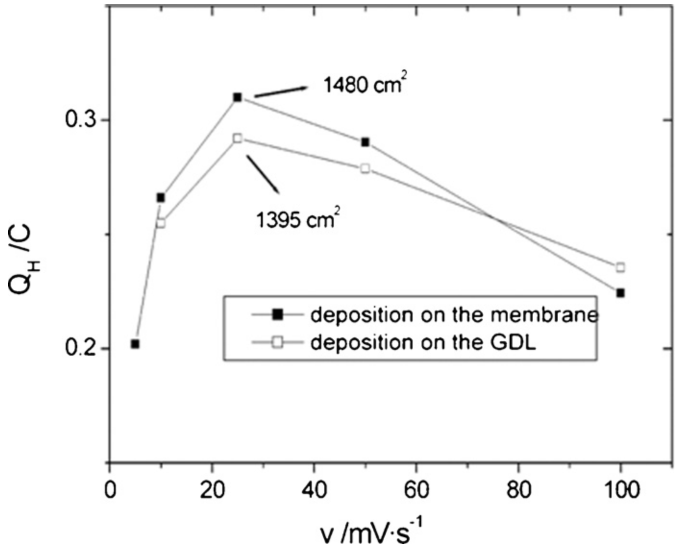

Fig. 7. Desorption H charge as a function of voltage sweep rate, measured for two catalyst layers deposited on the membrane and on the GDL. The electroactive area is calculated from the maximum value using 210 μC cm^{-2} conversion factor.

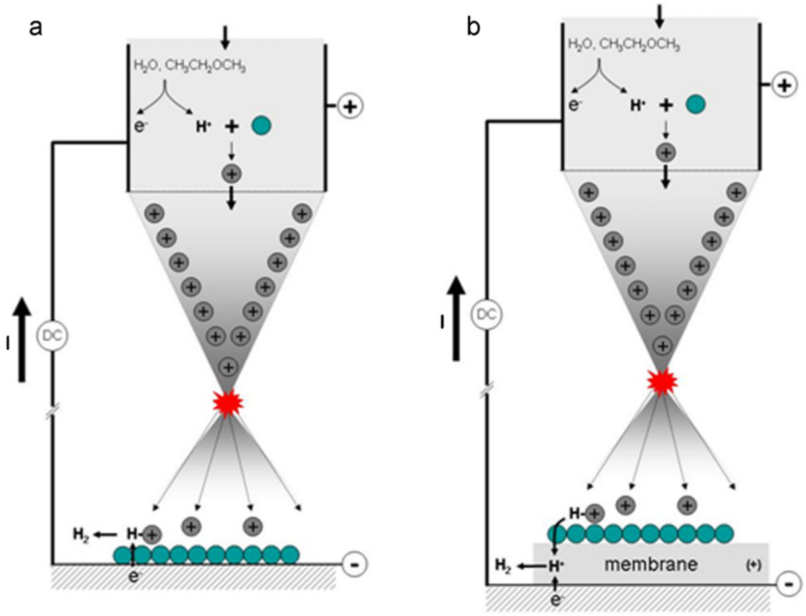

Fig. 8. Two schemes comparing electrospray deposition of catalyst layers on electronically conducting substrate (a), and proton conducting membrane (b).

into single aggregates, and partial breaking of Nafion side chains [19].

Once arriving at the substrate, charged particles and ionomer deposit under electrostatic interaction and discharge. On electronic conducting substrate, like GDL and Al foil, such process occurs by charge transfer to the substrate:

$$[\mathrm{P}]\text{–}\mathrm{BH}^+ + \mathrm{e}^- \rightarrow [\mathrm{P}]\text{–}\mathrm{B}: + 0.5\mathrm{H}_2 \tag{6}$$

However, the electronic exchange with the Nafion substrate is not possible. In this case, particles arriving to the Nafion membrane can only discharge by proton release:

$$[\mathrm{P}]\text{–}\mathrm{BH}^+ \rightarrow [\mathrm{P}]\text{–}\mathrm{B}: + [\mathrm{H}^+]_{\mathrm{Nf}} \tag{7}$$

After exchange, protons migrate through the membrane towards the back contact where they are electrochemically reduced:

$$[\mathrm{H}^+]_{\mathrm{Nf}} + \mathrm{e}^- \rightarrow 0.5\mathrm{H}_2 \tag{8}$$

The electrospray deposition process is schematised in Fig. 8, comparing now deposition on electronically conducting substrate and on proton conducting membrane. The main difference introduced by the substrate resides in the discharging mechanism by protons release and migration through Nafion (reactions (7) and (8)), which is more complex and slower, given the dry conditions of Nafion during deposition (typically under 30–40% ambient humidity), than the direct electron transfer on conducting substrate (reaction (6)). In addition, given the good dielectric properties of Nafion, the slow, proton mediated discharging may give rise to accumulation of positive charge in the membrane if the rate of ionized particles arrival is higher than the discharge. As a consequence, charging of the membrane will cause a change in the potential distribution and field intensity within the ejector–substrate gap. The possible influence of this effect on the electrospray process is further discussed in Appendix A.

4.2. Influence of Nafion substrate on the morphology of catalyst layers and single cell results

One of the interesting properties of the electrospray deposition is that the morphology of films can be controlled to a certain extent. There are few studies of the morphology of electrosprayed films as a function of experimental parameters. According to a droplet evaporation model applied to the growth of the polymer poly(vinylidene fluoride) (PVDF) [20], the most important variables controlling morphology are the growth rate, surface energy and shear rate of the droplet over the substrate. At low growth rates the morphologies are smoother if shear rate is high, whereas at high growth rate the morphology changes to more complicated shapes depending on the interplay of shear rate and interfacial energies. In a different study, platinum films deposited by electrospray show changes in microstructural properties as a function of platinum solution composition, temperature, ejector to substrate distance, solution flow rate and deposition time [21].

Substrate type is to our knowledge a parameter not studied in the electrospray deposition. It is clear that properties of the substrate like surface morphology, conductivity and dielectric constant must have an influence on the characteristics of the films, provided they are involved in the interaction of particles with the substrate, discharging mechanism and electric field distribution. On electronic conducting substrates, like GDL and Al, particles discharge by direct electronic exchange with the substrate (reaction (6)), giving rise to intensively ramified, dendritic, morphology. It is known that dendritic morphology in electrochemical deposition processes appear as a consequence of a heterogeneous distribution of current in those processes governed by electromigration of ions and/or diffusion limited aggregation [22–28]. The dendritic shape arises from the disposition of atoms under interplay of mass transfer and surface forces. In electrospray deposition on metallic substrate, particles arrangement is clearly under electromigration control and electrostatic interaction with the substrate, yielding conditions for a highly heterogeneous growth rate and the growth of dendritic shapes.

For electrospray deposition on membrane substrate, however, the dendritic growth is not favoured. The discharging of particles occurs by proton release and transport through the membrane towards the counter electrode (reactions (7) and (8)). This process may be slow and particle arrangement may be no longer under migration control. In addition, the electric field for electrospray is less intense if charge accumulation occurs in the membrane (see Appendix A). Such changes in electrospray conditions yield a change in the morphology of the film, from dendritic to globular: it is to be expected that particles arriving to the membrane will

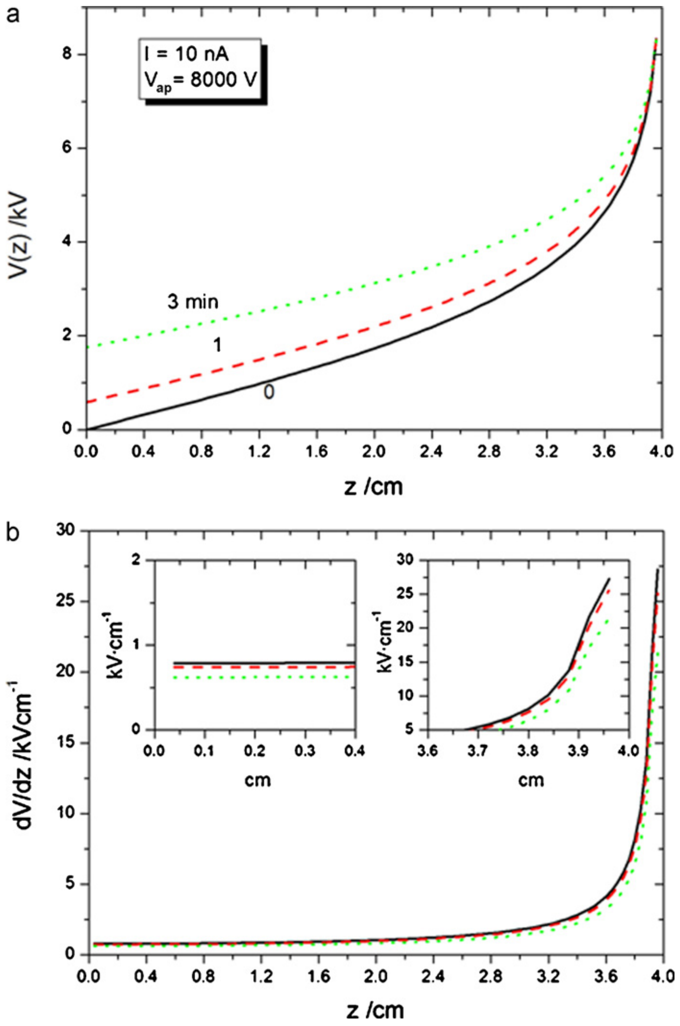

Fig. 9. (a) Potential distribution in the substrate ($z = 0$ cm) to needle ($z = 4$ cm) gap (axial direction, $r = 0$), after different electrospray deposition times with full accumulation of charge in the membrane. (b) Corresponding electric field intensity. Insets: details of the electric field in the close to the substrate and close to the needle areas.

have larger mobility (shear rate), and that non-electrostatic interactions may have higher influence, yielding an arrangement with smoother morphology [20]. The differences observed in the morphology of layers deposited close to the membrane with respect to the surface layers (Fig. 4), must be attributed to increased proton transport resistance with film thickness, yielding conditions more favourable for a smooth globular growth.

In spite of the differences in the morphology of the films, the properties of the catalyst layers in PEMFC electrodes appear little altered for the on-membrane deposition, as concluded from the analysis of the polarization curves (Table 1). Similar surface electroactive area values are measured for on-membrane and on-GDL cathodic layers, indicating optimal interaction between catalyst particles and ionomer phase in both cases. The main difference observed is in the high frequency resistance of the cell, which indicates that the protons conductivity between the catalyst layer and the membrane is considerably improved for on-membrane deposited catalyst films.

5. Conclusions

The preparation of catalyst layers by electrospray on Nafion membrane has been carried out. The layers result with good adherence, enough to maintain the integrity during post deposition processes. The globular morphology of the catalyst layers deposited on membrane, compared with the dendritic morphology of similar layers deposited on GDL, is attributed to a deposition process with slower particles discharge, mediated by proton release and conduction through the Nafion membrane. Single PEMFC testing shows that catalyst layers deposited on-membrane allow for lower internal resistance of the cell due to improved catalyst layer–membrane ionic contact.

Acknowledgments

This work has been carried out under Ministerio de Ciencia e Innovación, project DECATEL (Ref. MAT2007-64210), and Comunidad de Madrid program DIVERCEL, Ref. S-2009/ENE-1475.

Appendix A.

A.1. Electrospray conditions with membrane substrate

The Nafion membrane on top of the counter electrode modifies the potential profile in the needle to counter electrode space and causes changes in the electric field distribution. It is possible to estimate such changes in the light of basic principles and using available theoretical descriptions of electric field distribution with this particular electrodes disposition. The potential distribution in the needle to counter electrode space is highly non-uniform. The profile has been calculated by numerical methods [29,30], and also different analytical expressions have been proposed [31,32], yielding similar, although not the same, results, with the highest potential drop and field intensity close to the needle. For a view of the situation in the particular case of this work we take the analytical expression obtained by Jones and Thong. [31]:

$$V_{\mathrm{air}}(z) = V_{\mathrm{ap}} \frac{\log((z_0 - z)/(z_0 + z))}{\log(4z_0/r_n)} \tag{A.1}$$

where $V_{\mathrm{air}}(z)$ is the local potential in the axial direction, V_{ap} is the applied potential, z_0 is the distance from the needle tip to the counter electrode, and r_n is the needle radius. Fig. 9a and b shows the profiles of potential and electric field, respectively, with highest potential drop and electric field allocated close to the tip. By placing a thin, 50 μm thickness, Nafion layer on top of the counter electrode, the potential profile changes because the space between the needle and the counter electrode is now occupied by two dielectrics:

$$V_{\mathrm{ap}} = V_{\mathrm{air}} + V_{\mathrm{mem}} \tag{A.2}$$

where V_{mem} is the fraction of the applied potential drop inside the membrane. Under electrostatic conditions, an upper estimation of V_{mem} for a plane-to-plane potential distribution yields a very small fraction of the applied potential ($3 \times 10^{-4} V_{\mathrm{ap}}$, for Nafion of 50 μm thickness and 4 cm dielectrics gap). For a tip-to-plane disposition, the fraction is expected to be smaller given the large asymmetry of the potential profile, with the largest potential drop in the air close to the tip region.

The situation is different under electrospray current flow. The possibility of accumulation of charge in the membrane causes the potential drop V_{mem} to change in the following way:

$$V_{\mathrm{mem}} = \frac{Qd}{A\kappa\varepsilon_0} \tag{A.3}$$

Being Q ($=I \cdot t$) the charge stored in the membrane, d the membrane thickness, A the area, κ (=4) the dielectric constant, and ε_0 the free space permittivity. Fig. 9 compares the potential profiles under no charge flow and two different times, under 10 nA charging electrospray current and 15 cm^2 membrane area, and when there is complete accumulation of charge inside the membrane. It shows that the electric field intensity close to the tip may decrease by about 20% after 3 min total charge accumulation, which changes conditions for electrospray ionization. Close to the substrate a smaller decrease in the electric field takes place which may influence the disposition of particles on the substrate. However, conditions for a high accumulation of charge are probably not attained provided there is enough proton conductivity in the membrane and the interface with the back contact is properly done.

As a result it may be concluded that for electrospray on membrane, the electric field may decrease due to charge accumulation within the membrane, compare with the same conditions on a conducting substrate. A change in electric field intensity influences different parameters in the cone–jet mode, like cone shape, jet radius, current intensity, droplet size, and axial velocity [13,17,33]. Most important for film morphology may be particles velocity and surface interactions upon deposition. Lower electrostatic interaction at the membrane substrate, after a decrease in electric field intensity, favours the smooth, globular, morphology of catalyst films deposited on the membrane.

References

[1] R.B. Cole, J. Mass Spectrom. 35 (2000) 763–772.
[2] A. Jaworek, A.T. Sobczyk, J. Electrostat. 88 (2008) 197–219.
[3] S.J. Gaskell, J. Mass Spectrom. 32 (1997) 677–688.
[4] R. Benítez, J. Soler, L. Daza, J. Power Sources 151 (2005) 108–113.
[5] A.M. Chaparro, B. Gallardo, M.A. Folgado, A.J. Martín, L. Daza, Catal. Today 143 (2009) 237–241.
[6] A.M. Chaparro, M.A. Folgado, P. Ferreira-Aparicio, A.J. Martín, I. Alonso-Álvarez, L. Daza, J. Electrochem. Soc. 157 (2010) B993–B999.
[7] G.J. Van Berkel, V. Kertesz, Anal. Chem. 79 (2007) 5510–5520.
[8] M.S. Wilson, S. Gottesfeld, J. Appl. Electrochem. 22 (1992) 1–7.
[9] A. Lindermeir, G. Rosenthal, U. Kunz, U. Hoffmann, J. Power Sources 129 (2004) 180–187.
[10] H. Tang, S. Wang, M. Pan, S.P. Jiang, Y. Ruan, Electrochim. Acta 52 (2007) 3714–3718.
[11] A.M. Chaparro, A.J. Martín, M.A. Folgado, B. Gallardo, L. Daza, Int. J. Hydrogen Energy 34 (2009) 4838–4846.
[12] K.C. Neyerlin, W. Gu, J. Jorne, H.A. Gasteiger, J. Electrochem. Soc. 153 (2006) A1955–A1963.
[13] A.M. Gañán-Calvo, Phys. Rev. Lett. 79 (1997) 217–220.
[14] D. Hulicova-Jurcakova, M. Seredych, Y. Jin, G.Q. Lu, T.J. Bandosz, Carbon 48 (2010) 1767–1778.
[15] C. Poleunis, X.V. Eynde, E. Grivei, H. Smet, N. Probst, P. Bertrand, Surf. Interface Anal. 30 (2000) 420–424.
[16] R.P.A. Hartman, D.J. Brunner, D.M.A. Camelot, J.C.M. Marijnissen, B. Scarlett, J. Aerosol Sci. 30 (1999) 823–849.
[17] R.P.A. Hartman, D.J. Brunner, D.M.A. Camelot, J.C.M. Marijnissen, B. Scarlett, J. Aerosol Sci. 31 (2000) 65–95.
[18] F.-F. Hsu, J. Turk, J. Chromatogr. B 877 (2009) 2673–2695.
[19] A.M. Chaparro, R. Benítez, L. Gubler, G.G. Scherer, L. Daza, J. Power Sources 169 (2007) 77–84.
[20] I.B. Rietveld, K. Kobayashi, H. Yamada, K. Matsushige, J. Phys. Chem. B 110 (2006) 23351–23364.
[21] A. Lintanf, R. Neagu, E. Djurado, Solid State Ionics 177 (2007) 3491–3499.
[22] J.N. Chazalviel, Phys. Rev. A 42 (1990) 7355–7367.
[23] J.L. Barton, J.O'M. Bockris, Proc. R. Soc. Lond. A 268 (1962) 485–505.
[24] J.W. Diggle, A.R. Despic, J.O'M. Bockris, J. Electrochem. Soc. 116 (1969) 1503–1514.
[25] C. Monroe, J. Newman, J. Electrochem. Soc. 150 (2003) A1377–A1384.
[26] C. Gabrielli, L. Beitone, C. Mace, E. Ostermann, H. Perrot, J. Electrochem. Soc. 154 (2007) H393–H399.
[27] O. Crowther, A.C. West, J. Electrochem. Soc. 155 (2008) A806–A811.
[28] L.D. Rafailović, D.M. Minić, H.P. Karnthaler, J. Wosik, T. Trišović, G.E. Nauer, J. Electrochem. Soc. 157 (2010) D295–D301.
[29] S.S. Bamji, A.T. Bulinski, K.M. Prasad, IEEE Trans. Electr. Insul. 28 (1993) 420–424.
[30] X. Zhong, R. Yi, A.E. Holliday, D.D.Y. Chen, Rapid Commun. Mass Spectrom. 23 (2009) 689–697.
[31] A.R. Jones, K.C. Thong, J. Phys. D: Appl. Phys. 4 (1971) 1159–1168.
[32] G.-S. Chot, D.-E. Kim, S.-O. Kang, J. Phys. D: Appl. Phys. 23 (1990) 85–89.
[33] A.M. Gañán-Calvo, J.M. Montanero, Phys. Rev. E 79 (2009) 066305.